

Transverse coherent instability of a bunch in a rectangular potential well

V.Balbekov

*Fermi National Accelerator Laboratory
P.O. Box 500, Batavia, Illinois 60510**

(Dated: April 3, 2006)

Theory of transverse instability of a bunch in a rectangular potential well is developed. Series of equations adequately describing the instability is derived and solved both analytically and numerically. Dependence of the instability increment and threshold on bunch factor is investigated for various beam coupling impedances. The theory is applied to the Fermilab Recycler Ring.

PACS numbers: 29.20.-c, 29.27.Bd

I. INTRODUCTION

Fermilab Recycler is an antiproton storage ring with stochastic and electron cooling [1]. Transverse resistive wall instability is observed in the ring at intensity several $\times 10^{11} \bar{p}$ and relatively small phase volume of the bunch. A digital instability damper with high order filter is used increasing achievable phase density by a factor of about 2 [2, 3].

A distinctive feature of the Recycler is the RF system which can create a series of rectangular pulses (other possibilities are not considered here) [1]. A bunch of several microseconds long is kept in almost rectangular potential well which arises between two pulses of alternating polarity (barriers). Synchrotron frequency is very low in such a bucket (typically several Hz) having a 100% spread.

First theoretical analysis of resistive wall instability in the Recycler was published in Ref. [3]. It was shown that dependence of the instability decrement on bunch factor is rather moderate, and a coasting beam model was used to find the instability threshold.

More detailed investigation was performed in Ref. [4] where several impedances of different types were examined, including space charge and instability damper contributions. The problem was treated in terms of an effective impedance. It was shown that its real part (which is responsible for the instability) increases at the bunch squeezing not faster than its imaginary part. The permissibility of a coasting beam model for calculation of the instability threshold was confirmed by this.

However, a dependence of the increment or the effective impedance on a bunch factor was not established thoroughly in the mentioned articles. The basic challenge is a numerical calculation of high order eigenvalues of large matrices. Alternative method developed in this paper does not require a use of such cumbersome matrices, and allows to investigate the increment and threshold of very high eigenmodes. This is especially important for systems with an instability damper, where these modes

are most unstable.

We will consider a single bunch neglecting the penetration of particles into the barriers. Betatron oscillations are taken to be linear, because nonlinearity of external field is very small in the Recycler [1], and nonlinearity of space charge field does not affect the transverse oscillations of the beam center [5].

II. BASIC EQUATIONS

Let us consider the transverse dipole moment of a beam in its rest frame: $D(\theta) = \sum_k D_k \exp(ik\theta)$ where θ is longitudinal coordinate (azimuth), and dependence on time is presumed to be given by factor $\exp(-i\omega t)$. Then the Fourier coefficients D_k satisfy the following series of equations [4, 6]:

$$D_k = \frac{i r_0 \omega_0 N}{2\pi\gamma Q_0 Z_0} \sum_l C_{k,l}(\omega) Z_l(\omega) D_l \quad (1)$$

where $r_0 = e^2/mc^2$ (about 1.535×10^{-16} cm for protons), $Z_0 = 4\pi/c \simeq 376.7$ Ohm, N is the beam intensity, ω_0 and Q_0 are central angular velocity and betatron tune, respectively. Factors $Z_l(\omega)$ can be represented in terms of transverse beam coupling impedance in the laboratory frame, or in terms of the corresponding wake field [7]:

$$Z_k(\omega) = Z(\omega + k\omega_0) = i \int_0^\infty W(\theta) \exp\left(i\left[k + \frac{\omega}{\omega_0}\right]\theta\right) d\theta \quad (2)$$

The general formula for $C_{k,l}(\omega)$ is:

$$C_{k,l}(\omega) = \sum_m \int_0^\infty \frac{I_{m,k}(\nu, \epsilon) I_{m,l}^*(\nu, \epsilon) \mathcal{F}(\epsilon) d\epsilon}{\omega + \omega_0 Q_0 - m\Omega(\epsilon)} \quad (3)$$

where ϵ is longitudinal action and $\mathcal{F}(\epsilon)$ is corresponding normalized distribution function, $\Omega(\epsilon)$ is synchrotron frequency, $\nu = Q_0 - \xi/\eta$, ξ and η are the machine chromaticity and slippage factor, respectively. Form-factors

*Electronic address: balbekov@fnal.gov

$I_{m,k}(\nu, \epsilon)$ are the coefficients of expansion of a planar wave in series of multipoles:

$$I_{m,k}(\nu, \epsilon) = \frac{1}{2\pi} \int_{-\pi}^{\pi} \exp(im\phi - i[k - \nu]\theta(\epsilon, \phi)) d\phi \quad (4)$$

where the particle azimuth θ should be presented as a function of synchrotron action and phase.

III. RECTANGULAR POTENTIAL WELL

Now we have to apply these general formulae to the particles in a rectangular potential well of length $2\pi B$ where B is the bunch factor. Then Eq. (4) gives:

$$I_{m,k}(\nu) = 2iB[k - \nu] \frac{1 - \exp(i\pi[2B[k - \nu] - m])}{\pi[4B^2[k - \nu]^2 - m^2]}, \quad (5)$$

and the synchrotron frequency is:

$$\Omega = \frac{\omega_0|\epsilon\eta|}{8\pi p_0 B^2} = \frac{\omega_0|(p - p_0)\eta|}{2p_0 B} \quad (6)$$

where p is the particle momentum in the laboratory frame and p_0 is the central momentum of the beam [4]. Therefore, one can represent coefficients (3) of series (1) in the form:

$$C_{k,l}(\omega) = \sum_m I_{m,k}(\nu) I_{m,l}^*(\nu) \times \int_{-\infty}^{\infty} \frac{F(p) dp}{\omega + \omega_0 Q_0 - m\omega_0 \eta [p - p_0] / [2Bp_0]} \quad (7)$$

where $F(p)$ is the normalized distribution function on momentum.

Because the factors $I_{m,k}$ do not depend on action now, another form of series (1) can be proposed:

$$X_m = \frac{i r_0 \omega_0 N}{2\pi \gamma Q_0 Z_0} \sum_n Z_{m,n}(\omega) X_n \times \int_{-\infty}^{\infty} \frac{F(p) dp}{\omega + \omega_0 Q_0 - n\omega_0 \eta [p - p_0] / [2Bp_0]} \quad (8)$$

where

$$X_m = \sum_k Z_k(\omega) I_{m,k}^*(\nu) D_k, \quad (9)$$

and

$$Z_{m,n}(\omega) = \sum_k Z_k(\omega) I_{m,k}^*(\nu) I_{n,k}(\nu). \quad (10)$$

This form will be largely used for the analysis. Note that variables X_m can be treated as amplitudes of the longitudinal multipoles in the bunch spectrum.

IV. ZERO SLIPPAGE LIMIT

As it was mentioned above, the synchrotron frequency is extremely small in the Recycler Ring. Therefore, the limit $\Omega \rightarrow 0$ can be considered as a reasonable first approximation. Corresponding limiting process should not be performed by decreasing of the distribution width, because the effect of chromaticity would also be lost. It is necessary to proceed to the limit $\eta \rightarrow 0$ taking into account that $\nu \rightarrow \infty$ in this case. Then the dispersion equation following from series (1) is:

$$1 = \frac{i r_0 \omega_0 N Z_M^{(ef)}(\omega)}{2\pi \gamma Q_0 Z_0} \int_{-\infty}^{\infty} \frac{F(p) dp}{\omega + \omega_0 Q(p)} \quad (11)$$

where $Q(p) = Q_0 + \xi[p - p_0]/p_0$ is the momentum dependent betatron frequency [4]. The equation includes the effective impedance which is M -th eigenvalue of the series of equations:

$$Z_M^{(ef)}(\omega) D_k = \sum_l \rho_{k-l} Z_l(\omega) D_l \quad (12)$$

where

$$\rho_k = \frac{\sin(\pi B k)}{\pi B k} \exp(-i\pi B k), \quad (13)$$

are Fourier coefficients of the normalized linear density of the beam: $\rho(\theta) = 1/B$ at $0 < \theta < 2\pi B$. It is easy to see that $D_k = \delta_{k,M}$ and $Z_M^{(ef)}(\omega) = Z_M(\omega)$ at $B = 1$.

It can also be shown that for the rectangular potential well

$$\rho_{k-l} = \sum_m I_{m,k}(\nu) I_{m,l}^*(\nu). \quad (14)$$

This relation allows to obtain another form of series (12) corresponding to Eq. (8):

$$Z_M^{(ef)}(\omega) X_m = \sum_n Z_{m,n}(\omega) X_n. \quad (15)$$

One more form can be obtained by inverse Fourier transformation of series (12) resulting in the integral equation:

$$Z_M^{(ef)} D(\theta) = i\rho(\theta) \int_0^{\infty} D(\theta + \theta') W(\theta') \exp\left(\frac{i\omega\theta'}{\omega_0}\right) d\theta' \quad (16)$$

where $W(\theta)$ and $Z(\omega)$ are connected by Laplace transformation (2). Similar equation was applied earlier for an analysis of resistive wall instability in the Recycler [3].

V. EFFECTIVE IMPEDANCE

Several specific examples of effective impedance are considered below. Series (15) is used being the most convenient for numerical calculation. Its main advantage is

that the matrix $Z_{m,n}$ is nearly diagonal, which makes it possible to calculate eigenvalues by use of its rather small fragments. Note that the effective impedance does not depend on which value of ν is used for calculation of the matrix by Eq. (10), because the change produces unitary transformation of the matrix. In fact, all of the calculations below presume that $\nu = 0$. In addition, it is taken into account that $Z_{m,n} = Z_{-m,n} = Z_{m,-n}$ to reduce series (15) to the form:

$$Z_M^{(ef)}(\omega)X_m = \sum_{n=0}^{\infty} Z_{m,n}(\omega)X_n \quad (17)$$

where

$$Z_{m,n}(\omega) = \sum_k Z_k(\omega) I_{m,k}^*(0) I_{n,k}(0) \times \begin{cases} 1 & \text{at } n = 0 \\ 2 & \text{at } n > 0 \end{cases} \quad (18)$$

A. Exponential wake

Let us consider the wake field:

$$W(\theta) = -Z^{(exp)} \frac{\omega_f}{\omega_0} \exp\left(-\frac{\omega_f \theta}{\omega_0}\right) \quad (19)$$

and corresponding impedance in frequency domain:

$$Z(\hat{\omega}) = \frac{Z^{(exp)}}{\hat{\omega}/\omega_f + i} \quad (20)$$

(symbol 'hat' marks the laboratory frame). An analytical solution of the problem is possible in this case. In terms of Eq. (16), the eigenfunctions and the corresponding eigenvalues are:

$$D(\theta) = \rho(\theta) \times \exp\left(iK\theta + \left[i\frac{\omega + K\omega_0}{\omega_0} - \frac{\omega_f}{\omega_0}\right] \left[\int_0^\theta \rho(\theta')d\theta' - \theta'\right]\right), \quad (21)$$

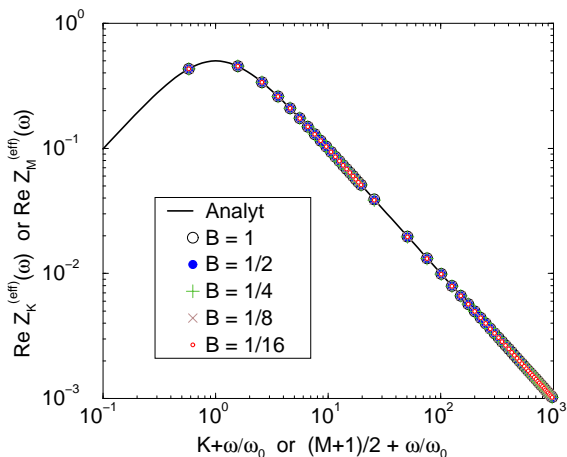


FIG. 1: Real part of exponential wake effective impedance. Numerical solutions are found at $\omega/\omega_0 = -0.425$.

and

$$Z_K^{(ef)}(\omega) = Z_K(\omega) = \frac{Z^{(exp)}}{(\omega + K\omega_0)/\omega_f + i}. \quad (22)$$

It is most remarkable that these eigenvalues do not depend on the bunch factor.

The eigenvalues of series (17) with positive real part are represented in Fig. 1 at $Z^{(exp)} = 1$, $\omega_f = \omega_0$, being calculated by the following method. At any B , first 20 of them are obtained with the help of 100×100 matrix $Z_{m,n}$ starting from 0-th multipole. Each other point is the first eigenvalue of a 10×10 matrix starting from multipole 50, 100, ..., 2000. The number M is defined as the index of the highest power multipole in the spectrum of the eigenmode. Note that only odd M appear in Fig. 1 because real parts of the eigenvalues are found to be negative otherwise. Many symbols in the figure overlap confirming that the eigenvalues do not depend on B .

According to Eq. (22), all of the eigenvalues should be located on the solid line plotted in Fig. 1. This is so indeed, and there is a perfect agreement of numerical and analytical solutions at the relation:

$$K = \frac{M+1}{2}. \quad (23)$$

A very important conclusion follows from these results: any eigenmode includes a rather small number of multipoles, and reasonable accuracy can be reached by using 10×10 or an even smaller fragment of the matrix $Z_{m,n}$. The conclusion will be applied below to more complicated impedances when analytical solution is not achievable.

B. Resistive wall impedance

The same technique is used in this subsection to calculate the effective resistive wall impedance:

$$Z(\hat{\omega}) = Z^{(rw)} [\text{sgn}(\hat{\omega}) - i] \sqrt{\left|\frac{\omega_0}{\hat{\omega}}\right|}. \quad (24)$$

The results at $Z^{(rw)} = 1$ are shown in Fig. (2) and are fitted by the formula:

$$\begin{aligned} Z_M^{(eff)}(\omega) &= \frac{1}{\sqrt{B}} Z\left(\omega + \frac{\omega_0[M+1]}{2}\right) \\ &= \frac{1}{B} Z\left(\frac{\omega}{B} + \frac{\omega_0[M+1]}{2B}\right). \end{aligned} \quad (25)$$

At $B = 1$, the fit coincides with analytical solution of Eq. (12) if relation (23) is also applied. At arbitrary B and $M \gg 10$, rather good agreement is provided by the expression:

$$Z_M^{(eff)}(\omega) \simeq \frac{1}{B} Z\left(\frac{\omega_0 M}{2B}\right). \quad (26)$$

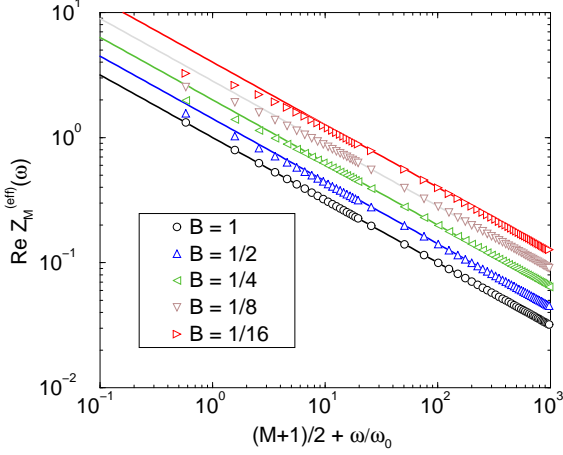


FIG. 2: Real part of resistive wall effective impedance. Solid lines represent fit (25).

However, the agreement is worse at lower M . In particular, better approximation for the lowest unstable mode is:

$$Z_1^{(ef)} \simeq \frac{Z^{(rw)}[1-i]}{B^{1/3}\sqrt{K-Q_0}} \quad (27)$$

where K is the minimal integer exceeding Q_0 .

C. Resistive wall + first order damper

At imaginary $Z^{(exp)}$, impedance (20) represents the simplest model of an instability damper with first order RC filter (imaginariness is actually provided by appropriate arrangement of pickup, kicker, and delay line). We

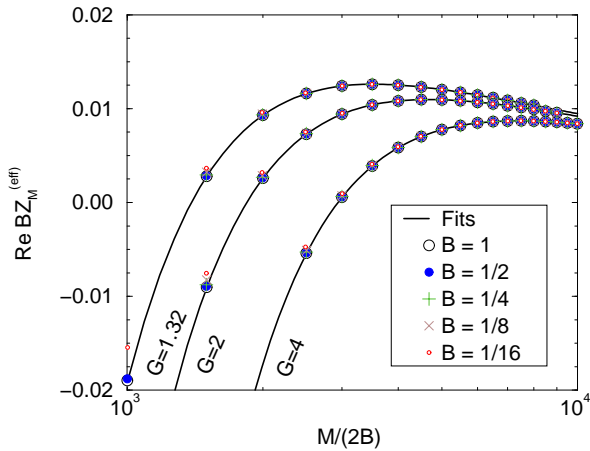


FIG. 3: Real part of resistive wall + 1st order damper effective impedance.

consider it jointly with resistive wall contribution representing the full impedance in the form:

$$Z(\hat{\omega}) = Z^{(rw)} \left[\text{sgn}(\hat{\omega}) - i \right] \sqrt{\left| \frac{\omega_0}{\hat{\omega}} \right|} - \frac{iG}{\hat{\omega}/\omega_f + i} \quad (28)$$

The effective impedances are calculated with the help of 10×10 matrix starting from M -th multipole at $Z^{(rw)} = 1$, $\omega_f/\omega_0 = 200$ and several G . Their real parts are shown in Fig. 3 in the area of rather large M , where positive values appear for the first time. Fits obtained using Eq. (26) and (28) are plotted as well, providing very good agreement for positive values.

D. Resistive wall and high order damper

The impedance

$$Z(\hat{\omega}) = Z^{(rw)} \left[\text{sgn}(\hat{\omega}) - i \right] \sqrt{\left| \frac{\omega_0}{\hat{\omega}} \right|} - \left[\frac{\sin(\pi\hat{\omega}/\omega_s)}{\pi\hat{\omega}/\omega_s} \right]^2 \begin{cases} G & \text{at } |\hat{\omega}| < \omega_f \\ 0 & \text{at } |\hat{\omega}| > \omega_f \end{cases} \quad (29)$$

is considered in this subsection. At non-integer ω_s/ω_0 , the addition to resistive wall part can be interpreted as a simple model of digital damper with sampling frequency ω_s and high order filter of bandwidth ω_f [8]. The case $G = 5/3$, $\omega_s/\omega_0 = 588.1$, $\omega_f = \omega_s$ is plotted in Fig. 4. Again, the numerical values are fitted very well by Eq. (26). Similar results are obtained at $\omega_f < \omega_s$ as well.

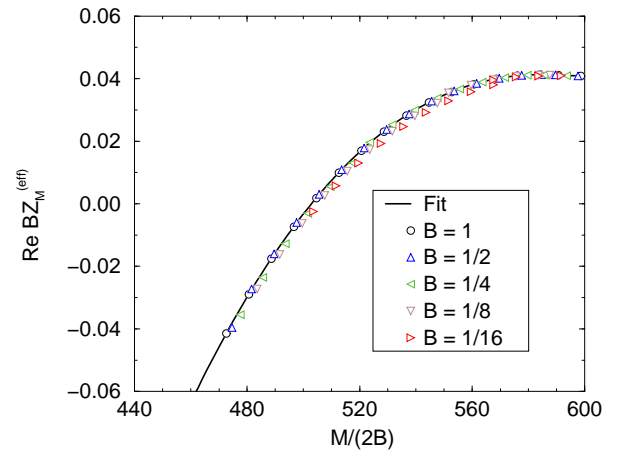


FIG. 4: Real part of resistive wall + high order damper effective impedance.

VI. INCREMENT OF THE INSTABILITY

According to Eq. (11), at relatively small momentum spread the instability increment is:

$$\text{Im } \omega = \frac{r_0 \omega_0 N}{2\pi\gamma Q_0 Z_0} Z_M^{(ef)}(-\omega_0 Q_0). \quad (30)$$

As shown in the previous section, its dependence on bunch factor is rather diverse. For the most unstable modes the obtained results can be summarized as:

- Exponential wake: no dependence on B ;
- Resistive wall: approximately $\propto B^{-1/3}$;
- Resistive wall + high frequency damper: $\propto B^{-1}$.

In the last case the increment depends on local beam density only, which means that the instability is driven by a short-range interaction. This fact can be explained by taking into account that the bunch spectrum includes a relatively small number of high order multipoles in this case, concentrating near $M \sim 2B\omega_f/\omega_0$. Another important point is an intimate connection of the multipoles and space harmonics due to the relation $\theta = 2B|\phi|$. As a result, the beam spectrum of any unstable mode in laboratory frame includes frequencies $\sim \omega_f \pm \Delta\omega$ where $\Delta\omega < \sim \omega_0/B$ arises because of the bunching. At $\omega_f \gg \omega_0/B$, only high-frequency harmonics are present in the spectrum. Typically, they are rather quickly damped out, resulting in a suppression of long-range interaction.

Similar reasoning could be applied to any high order mode (though it is unobservable in practice). Being consistent with Eq. (26) for resistive wall instability, this statement contradicts – from the first glance – the exponential wake effective impedance (22) because the last does not depend on the bunch factor. In fact, there is no contradiction here because the statement is related to high modes, i.e. to high frequency only. Then it follows from (20) and (22):

$$Z^{(ef)}(\omega) = Z(\omega) \propto 1/\omega \propto Z(\omega/B)/B$$

in total agreement with Eq. (26).

VII. THRESHOLD OF THE INSTABILITY

Frequency independent space charge impedance $Z = -iZ^{(sc)}$ should be taken into account when the instability threshold is calculated, because it usually produces a determining effect on Landau damping. Using Eq. (18), it is easy to verify that the inclusion provides an additive contribution $-iZ^{(sc)}/B$ to all diagonal elements of the matrix $Z_{m,n}$, i.e. to all its eigenvalues. For example, threshold of the lowest (most unstable) mode of resistive wall instability should be determined from Eq. (11) where

$$Z_1^{(ef)} = \frac{Z^{(rw)}[1-i]}{B^{1/3}\sqrt{K-Q_0}} - \frac{iZ^{(sc)}}{B} \quad (31)$$

and minimal $K > Q_0$ is applied. Absence of slippage factor in this case is actually immaterial, because its contribution to frequency spread would be small in comparison with chromaticity contribution.

However, the slippage can be important for the analysis of a wide-band damper, because fast-modulated eigenmodes with dominant contribution of higher multipoles are most unstable in this case. Fortunately, this drawback can be easily remedied due to the narrowness of the eigenmode spectrum discussed above. It is sufficient to separate corresponding central multipoles $n = \pm M$ in Eq. (8) and to retain them in all following transformations. Next, taking into account also Eq. (6) and relation $F(p-p_0) = F(p_0-p)$, the following equation can be obtained instead of Eq. (11):

$$1 = \frac{ir_0\omega_0 N Z_M^{(ef)}(\omega)}{2\pi\gamma Q_0 Z_0} \int_{-\infty}^{\infty} \frac{F(p) dp}{\omega + \omega_0 Q(p) + M\omega_0 \eta [p-p_0]/2Bp_0}. \quad (32)$$

This expression can be represented in the form very similar to the coasting beam dispersion equation:

$$1 = \frac{ir_0\omega_0 N Z^{(ef)}(\hat{\omega})}{2\pi\gamma Q_0 Z_0} \int_{-\infty}^{\infty} \frac{F(p) dp}{\hat{\omega} - \omega_r(p)[\kappa - Q(p)]} \quad (33)$$

where $\omega_r(p)$ is angular velocity of a particle with momentum p in the laboratory frame, $\hat{\omega} = \omega + \kappa\omega_0$, $\kappa = M/2B$. An appropriate form of the effective impedance should be used in this equation. For example, substitution of Eq. (31) allows to find threshold of resistive wall instability. When the higher modes are considered, Eq. (26) should be used resulting:

$$Z^{(ef)}(\hat{\omega}) = \frac{Z(\hat{\omega})}{B}, \quad (34)$$

where $Z(\hat{\omega})$ is total beam coupling impedance, including space charge contribution, resistive wall, damper, etc.

Gaussian distribution function F with dispersion σ is considered below. Then all the solutions of Eq. (33) are stable ($\text{Im } \omega \leq 0$) at the condition:

$$\left| \frac{\text{Re } \Delta\omega}{\delta\omega} \right| < f \left(\left| \frac{\text{Re}(\Delta\omega)}{\text{Im}(\Delta\omega)} \right| \right) = f \left(\left| \frac{\text{Im}(Z^{(ef)})}{\text{Re}(Z^{(ef)})} \right| \right) \quad (35)$$

where $\Delta\omega$ is the impedance produced frequency shift:

$$\Delta\omega = \frac{ir_0\omega_0 N Z^{(ef)}}{2\pi\gamma Q_0 Z_0}, \quad (36)$$

$\delta\omega$ is the r.m.s. frequency spread due to the momentum spread:

$$\delta\omega = \left| \xi + \eta[\kappa - Q_0] \right| \frac{\omega_0 \sigma}{p_0}, \quad (37)$$

and function f is represented by solid line in Fig. 5. A

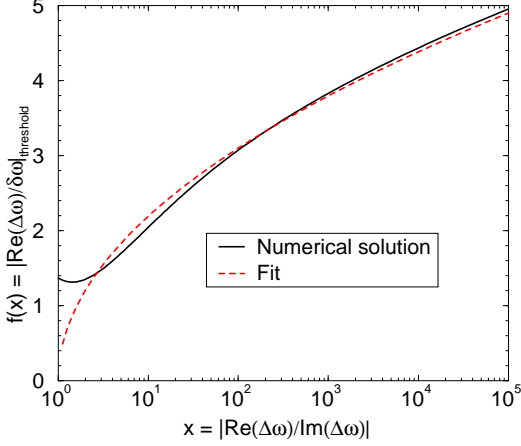


FIG. 5: Plot to calculate threshold of instability at Gaussian distribution.

simple fit

$$f(x) \simeq \sqrt{4.8 \log(x)} \quad (38)$$

is also plotted providing rather good approximation at $x > 3$.

The space charge impedance often dominates among others, so that imaginary part of the total impedance significantly exceeds its real part. If the beam transverse distribution function is Gaussian, the statement can be written in the form:

$$|\text{Re } Z^{(ef)}| \ll |\text{Im } Z^{(ef)}| \simeq \frac{Z^{(ch)}}{B} = \frac{\pi Z_0 Q_0}{4BS_{\perp}\beta\gamma} \quad (39)$$

where and S_{\perp} is transverse normalized r.m.s. phase volume of the beam [5]. Then stability condition (35) can be represented in the form:

$$\frac{N}{S_{\parallel}S_{\perp}} < \frac{4\omega_0\gamma|\xi + [\kappa - Q_0]\eta|}{\pi\beta e^2} f\left(\left|\frac{\pi Q_0 Z_0}{4\beta\gamma S_{\perp} B \text{Re}(Z^{(ef)})}\right|\right) \quad (40)$$

where

$$S_{\parallel} = BC\sigma \quad (41)$$

is treated as longitudinal r.m.s. phase volume of the bunch, and C is the machine circumference.

VIII. EXAMPLE: FERMILAB RECYCLER

We continue the analysis taking the Fermilab Recycler Ring as an example with the following parameters:

- $\omega_0 = 2\pi \times 89.86$ kHz
- $\gamma = 9.526$
- $\xi = -(2 \div 6)$

- $\eta = -0.0085$
- $Q_0 = 25.425$

Then Eq. (40) and (38) give the condition of stability:

$$D \equiv \frac{N/10^{10}}{4S_{\parallel}(\text{eV-s}) 6S_{\perp}(\pi\text{-mm-mrad})} < 0.14 \left| \xi - 0.0085[\kappa - Q_0] \right| \sqrt{\log \left| \frac{0.66\pi Z_0}{S_{\perp} B \text{Re}(Z^{(ef)})} \right|} \quad (42)$$

where 95% emittances are used in the definition of space phase density D . Some special cases are considered below:

A. Resistive wall impedance

This impedance is the main source of instability in the Recycler. Characteristic parameter $Z^{(rw)} \simeq 18$ MOhm/m [2, 4] provides for the lowest (most unstable) mode:

$$\text{Re } Z_1^{(ef)} \simeq \frac{24(\text{MOhm/m})}{B^{1/3}}. \quad (43)$$

Because slippage is negligible in this case, Eq. (42) gives:

$$D < 0.14 |\xi| \sqrt{\log \left(\frac{10}{S_{\perp} B^{2/3}} \right)}. \quad (44)$$

It means that the beam becomes more stable at the squeeze, though the dependence is very weak, and estimation $D < \sim 0.14 |\xi| \simeq 0.3 \div 0.8$ is valid at $S_{\perp} \sim 1$ π -mm-mrad and any reasonable B .

B. Resistive wall + first order damper

As it is shown in subsection V.C, at $\omega_f \gg \omega_0$ and $\kappa \gg 1$ the real part of total effective impedance is:

$$\text{Re } Z^{(ef)} = \frac{18(\text{MOhm/m})}{B} \left[\frac{1}{\sqrt{\kappa}} - \frac{G}{1 + \omega_0^2 \tau^2 \kappa^2} \right]. \quad (45)$$

This value becomes positive at $\kappa > \kappa_0 \simeq [G/\omega_0^2 \tau^2]^{2/3}$, but the beam still remains stable at the condition:

$$D < 0.14 \left| \xi - 0.0085\kappa \right| \sqrt{\log \left(\frac{14\sqrt{\kappa}}{S_{\perp} [1 - (\kappa_0/\kappa)^{3/2}]} \right)} \quad (46)$$

which does not depend on the bunch factor. In dependence on κ_0 , the right-hand part reaches a minimum (the beam becomes most unstable) at $\kappa \simeq (1.05 \div 1.10)\kappa_0$. A substitution to Eq. (46) results in the expression

$$D_{min} \simeq 0.28 |0.009\kappa_0 - \xi| \quad (47)$$

which provides acceptable accuracy at $S_{\perp} = 1$ π -mm-mrad. For example, at $G = 4$ and $\omega_f/\omega_0 = 200$ (18 MHz filter) $\kappa_0 \simeq 2950$, i.e. $D_{min} \simeq 0.28 |27 - \xi| = 8.1 \div 9.2$.

C. Resistive wall + high order damper

As it is shown in subsection V.D, at $\omega_f \gg \omega_0$ and $\kappa \gg 1$ real part of the total effective impedance is:

$$\text{Re}(Z^{(ef)}) = \frac{18 \text{ (M}\Omega\text{m/m)}}{B} \times \left[\frac{1}{\sqrt{\kappa}} - \left[\frac{\sin(\pi\kappa\omega_0/\omega_s)}{\pi\kappa\omega_0/\omega_s} \right]^2 \begin{cases} G & \text{at } |\kappa\omega_0| < \omega_f \\ 0 & \text{at } |\kappa\omega_0| > \omega_f \end{cases} \right]. \quad (48)$$

With reasonable accuracy, ultimate beam density can be found by the expression:

$$D_{min} \simeq 0.22 \left| 0.0086 \frac{\omega_f}{\omega_0} - \xi - 0.25 \right| \quad (49)$$

which does not depend on the gain (however, $G > 1.3$ is required to ensure suppression of the lowest mode). It gives $D_{min} \simeq 0.22 |3.2 - \xi| = 1.1 \div 2.0$ at $\omega_f/\omega_0 = 400$ (present situation [2]), and $D_{min} \simeq 0.22 |4.8 - \xi| = 1.5 \div 2.4$ at $\omega_f/\omega_0 = \omega_s/\omega_0 = 588.1$.

IX. CONCLUSION

It is shown that the transverse instability of a rectangular bunch can be described by the same dispersion equation as a coasting beam, if an effective beam coupling impedance is used instead of the standard one. Several methods to calculate the effective impedance are considered: integral equation for the beam dipole moment, corresponding series of equations for Fourier harmonics, or equivalent series for amplitudes of multipoles. The last method is most universal and convenient for a numerical solution because corresponding matrix is approximately diagonal. This property allows to use relatively small fragments of the matrix to calculate its eigenvalues including high order ones, starting from desirable number and scanning step by step the whole matrix. This also means that any eigenmode includes a rather small number of multipoles and has a narrow-band spec-

trum. In particular, it follows from this that the spectrum of high order eigenmodes includes only high frequencies which typically damp sufficiently rapidly to exclude long-range interaction in the beam. Therefore the effective impedance of these modes is proportional to B^{-1} , and high-frequency collective effects depend only on local linear density of the beam (however it is important that the density is constant within the whole bunch). Dependence of the effective impedance on B is diverse for lower modes, but typically it increases at the bunch squeezing. For example, effective resistive wall impedance $\propto B^{-1/3}$ for the most unstable mode.

Being applied to the Fermilab Recycler, the theory gives achievable beam density summarized in the table below (see Eq. (42) for the units). Numbers in brackets are achievable beam intensities in units of 10^{10} at the phase volume $4S_{\parallel} \times 6S_{\perp} = 70 \text{ eV-s} \times 7 \pi\text{-mm-mrad}$.

TABLE I: Achievable Recycler beam density and intensity.

Chromat.	A ^a	B ^b	C ^c	D ^d
-2	0.3 (150)	1.1 (550)	1.5 (750)	8.1 (4000)
-6	0.8 (400)	2.0 (1000)	2.4 (1200)	9.2 (4500)

^aNo damper

^bDigital damper 35 MHz

^cDigital damper 53 MHz

^dAnalog damper 18 MHz

High frequency related results should be valid for multi-bunch regime as well, restricting parameters of any bunch. However, they cannot be applied to very short bunches when penetration of particles into the barriers becomes essential. Beam shaping before extraction (“mining”) is an example of such a regime, when a multi-pulse RF wave form is generated without any space between the pulses. Then potential wells are triangular, and the results break down. The possibility must not be ruled out that the threshold decreases and instability appears at the mining, which effect could explain the slow transverse emittance growth observed in the Recycler at the mining [9].

[1] Gerry Jackson, FERMILAB-TM-1991 (1996).
 [2] J. L. Crisp, M. Hu, V. Tupikov, in *Proceeding of the 2005 Particle Accelerator Conference, Knoxville, TN, USA, 2005*, p. 1239
 [3] A. Burov and V. Lebedev, AIP Conf. Proc.773: 350-354, 2005.
 [4] V. Balbekov, in *Proceeding of the 2005 Particle Accelerator Conference, Knoxville, TN, USA, 2005*, p. 2567

[5] V. Balbekov, FERMILAB-FN-0782-AD, 2006.
 [6] F. Sacherer, CERN-SI-BR-72-5, 1972.
 [7] A. Piwinski, DESY 94-068, 1994.
 [8] V. Balbekov, FERMILAB-FN-0783-AD, 2006.
 [9] L. Prost et.al. <https://beamdocs.fnal.gov/DocDB/0020/002035/001/113005/EmitGrowthUpdate.ppt>, 2005.